Available online at www.sciencedirect.com
SCIENCE DIRECT®
Journal of Applied Geophysics 54 (2003) 97–109
JOURNAL OF APPLIED GEOPHYSICS
www.elsevier.com/locate/jappgeo

Joint inversion of Wenner and dipole–dipole data to study a gasoline-contaminated soil

Matías de la Vega[1], Ana Osella*[,1], Eugenia Lascano

Dpto. de Física, Fac. Cs. Exactas y Naturales, Gr. Geofis. Aplicada, Universidad de Buenos Aires, Ciudad Universitaria, Pab. 1-1428, Buenos Aires, Argentina

Received 24 April 2002; accepted 26 August 2003

Abstract

The goal of this work was to study a contaminated soil due to a gasoline spill produced by fissures in a concrete purge chamber located along a gas transmission line. A monitoring well drilled 16 m down gradient from the purge chamber revealed the presence of a gasoline layer of 0.5 m thick at 1.5 m depth, floating on top of the water table. A second well, drilled 30 m away from the first well, and in the same direction, did not show any evidence of contamination. To investigate this problem, a geoelectrical survey was conducted, combining dipole–dipole and Wenner arrays. First, four dipole–dipole profiles in a direction perpendicular to the longitudinal axis joining the wells were carried out. The electrical tomographies obtained from the 2D inversion of the data showed that the contaminated region was *characterized by a resistive plume* located at a depth between 1 to 2 m and had lateral extent of about 6–8 m. The longitudinal extension was less than 20 m, since the last profile located 30 m farther from the chamber did not show this kind of anomaly. To better determine the longitudinal extension, we performed a dipole–dipole profile along a line in this direction. The inverse model confirmed that the extension of the contaminated section was about 16 m. To complete the study of the deeper layer, we carried out Wenner soundings. The results of the inversion process indicated that to a depth of 20 m the soil was very conductive, because of the presence of clays as the main constituents, which confine the contaminant within this impermeable surrounding. To improve the inverse model, we performed a joint inversion of dipole–dipole and Wenner data. Analysis of the depth of penetration showed that it increased to 25 m and comparing the resulting model with the ones obtained from each array separately, we concluded that the joint inversion improves the depth *obtained* by the survey, while maintaining the shallow lateral resolution.

Keywords: Oil contamination; Resistivity methods; Joint inversion

1. Introduction

A priority of groundwater management is the protection of water quality in an aquifer. There are many artificial sources of potential groundwater contamination, and one of the most important is concerned with pollution due to hydrocarbon exploitation, in particular, during the transmission of the different products such as crude oil, gasoline, liquefied petroleum gas, and natural gas liquids along underground systems. Although the pipelines are designed to retain their contents, many leak to some extent. Weaknesses in the isolation appear also at

* Corresponding author. Fax: +54-1-782-7647.
E-mail address: osella@df.uba.ar (A. Osella).
[1] Also at Consejo Nacional de Investigaciones Científicas y Técnicas (CONICET).

0926-9851/$ - see front matter © 2003 Elsevier B.V. All rights reserved.
doi:10.1016/j.jappgeo.2003.08.020

sewers and purge chambers, especially the old ones. Both steel structures, subjected to corrosion, and concrete chambers, which can contain fissures, can develop spills with the consequent contamination of the subsoil. The contaminants combine with groundwater, and flow into the ground with the additional risk that this contaminated groundwater can move from one aquifer to another.

Once a spill has been detected, a number of matters should be addressed before the techniques for site remediation can be applied. The first one is the detection of the source of contamination to prevent the continuing release of the contaminants. Then, it is necessary to know how contaminants disperse and distribute in the subsurface, and what the characteristics of the surrounding media are. This knowledge is used to evaluate the probability that the contaminant may reach an aquifer, and also to determine if there is a possible conduit for the flow to other aquifers. Answers to all these aspects are required to determine the adequate methods for soil and aquifer remediation.

One way to characterize a contaminated zone is through the electrical resistivity of the soil. Hydrocarbons have in general much *higher* resistivity than water, *as such* the contaminant plume can be detected as a high resistivity anomaly. Results of these characteristics have been reported in many works (e.g., Endres and Greenhouse, 1996; Benson et al., 1997; Buselli and Lu, 2001).

On the other hand, different studies have shown an increase in the electrical conductivity in oil polluted zones associated to the biodegradation processes (e.g., Fetter, 1993; Sauck et al., 1998; Atekwana et al., 2000). This increase in the electrical conductivity could be the result of enhanced mineral weathering due to acids produced during the biodegradation of organic molecules (Sauck, 2000). A fact to be taken into account is the time scale, which is also an indicator of the evolution of the degrading process; recent spills should be resistive but with time as biodegradation proceeds, the contaminant plume should become more conductive (Sauck, 1998; 2000).

Thus, to properly describe the contaminant plume through the interpretation of geoelectrical data, the results should be combined with data from control wells in order to properly identify its electrical behavior. In this way, resistivity methods could act as a reliable diagnostic method to estimate the degree and extent of the contaminated soil.

In 2001, we began a project to characterize soils contaminated by hydrocarbons due to spills from purge chambers located along a gas transmission system located in Patagonia, south Argentina. These chambers are used to recover gasoline from the gas flowing along pipelines and are distributed usually every 2 or 3 km. Control wells located close to them revealed the presence of contaminants, indicating the existence of fissures or defects in the isolation covers on many of them. In previous work (Osella et al., 2002), we presented the first results corresponding to one of these chambers. In that case, data from control wells showed the presence of a 1.5-m-thick layer of gasoline floating over the water table at 7 m depth. In the case presented here, data from control wells revealed a 0.5-m-thick layer of gasoline at a depth of 1.5 m floating on the water table. As the objective of the work was not only the characterization of the subsoil to determine the contaminant plume extent but also to give information for future remediation, we had to extend the area under study following the slope of the ravine. Thus, the survey design required covering a zone of approximately 40×140 m with deep penetration and at the same time optimizing the resolution of the shallow layers. To obtain this combination, we used dipole–dipole and Wenner configurations. We used the data from the control wells to identify the contaminant plume and determine its electrical signature. Finally, we performed a joint inversion of dipole–dipole and Wenner data to better localize and characterize both the contaminant lens and its environment.

2. Site description

The purge chamber (Fig. 1) is located in the middle of a ravine. In this region, the water table *appears confined in small sand lenses within a clay environment* (Grizinik, 2000). A control well, WA, drilled 16 m down gradient from the chamber detected a 0.50-m-thick gasoline layer floating over the water table at a depth of 1.5 m. The stratigraphy of the well confirmed a soil formed mainly by clays up to a depth of 9 m. A second well, WB, was drilled 30 m away, following the direction of the surface slope,

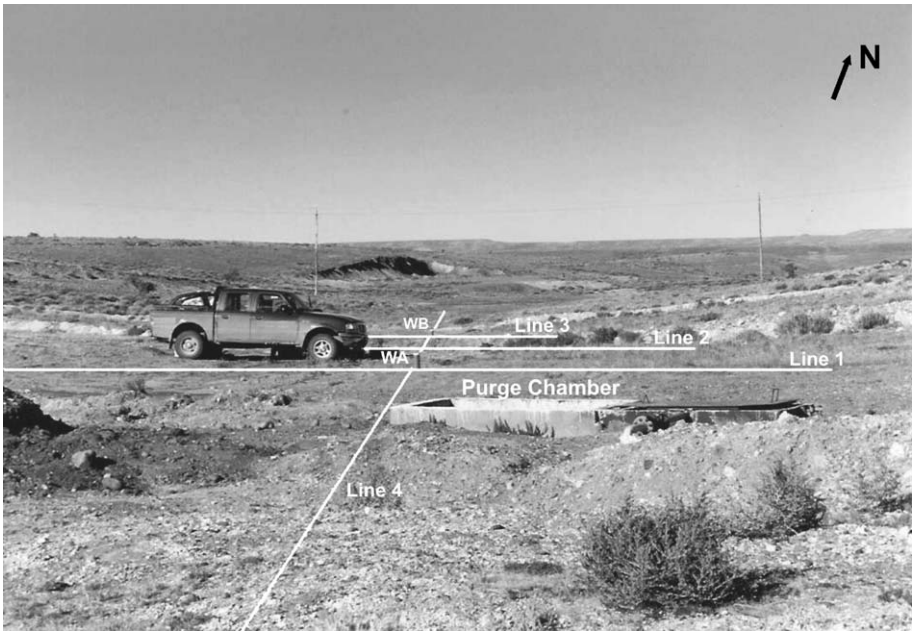

Fig. 1. View of the purge chamber and surrounding area. The lines indicate the approximate location of the profiles; wells WA and WB are also shown.

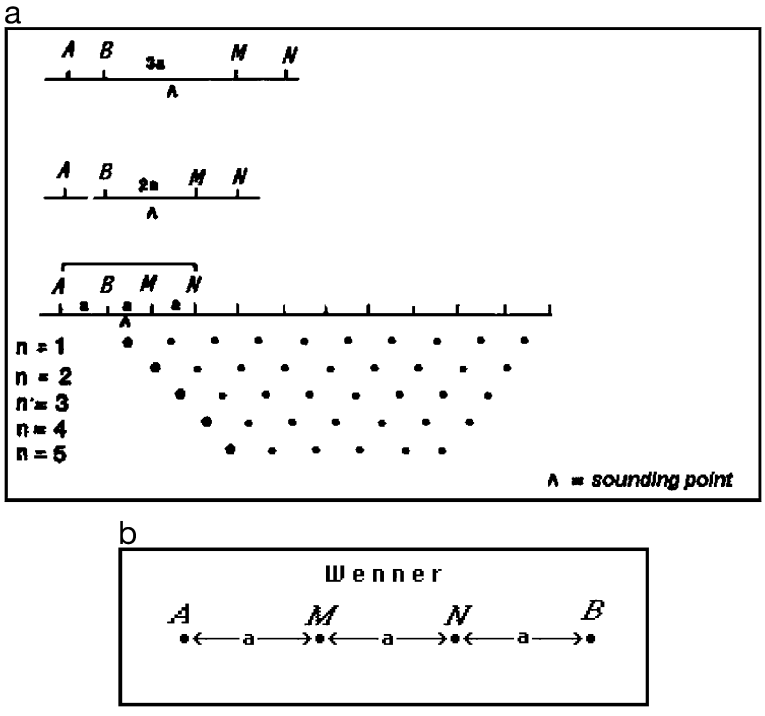

Fig. 2. Sounding configurations, (a) dipole–dipole configuration, (b) Wenner configuration. A and B correspond to the injection current electrodes while M and N are the potential electrodes (Reynolds, 1998).

which coincides with a riverbed which is dry at present. No water was detected at the time of the drilling but, after 5 days, the level reached approximately 0.8 m, without any evidence of gasoline. Further analyses confirmed that dissolved gasoline was not present, suggesting that the contaminated zone could be confined in a small zone close to the chamber. The chemical analysis indicated water rich in bicarbonates and with low salinity.

3. Methodology

To delineate the extent of the contaminant plume and to discount the possibility of interconnection with another aquifer or porous sandy lens contained in the clay medium, we conducted the geoelectrical survey, covering a 40 × 140 m area.

The zone in which the purge chamber was located is a ravine and because of this we chose two directions for the profiling, one perpendicular to its axis and one parallel to it. To achieve better lateral resolution, we first applied the dipole–dipole configuration (see Fig. 2a) to obtain the apparent resistivity pseudosections and their corresponding resistivity sections. In this way, we could determine the contaminant lens extent. Once the contaminated lens extent was determined, we used the Wenner configuration (see Fig. 2b) to characterize the zone surrounding it. It has to be taken into account that the depth of penetration of a sounding depends on the electrode separation in addition to the electrical properties of the medium. For dipole–dipole arrays, this depth depends on the value of *na* (see Fig. 2a) while for Wenner soundings it is related to the value of AB/2 (Fig. 2b). The penetration increases as these parameters increase (see e.g., Reynolds, 1998).

Data were collected with a multielectrode deployment. An HPE3612A DC power supply was used to inject current and measurements were collected using a data acquisition system that allows readings with a precision of 0.33 μV.

To analyze the data of each profile, we used the DCIP2D inversion code developed by the University of British Columbia (UBC) and based on the works of Oldenburg et al. (1993) and Oldenburg and Li (1994). A measure of the quality of the inversion process is given by the misfit, i.e., the distribution of the difference between the observed and predicted data, normalized by the standard deviation.

It is known that inversion problems are not unique. A way to improve the application of these techniques is to determine which parts of the model obtained from the inversion of the field data are real representations of the features of the subsoil. To do this, the depth reached by the profile should be estimated. The depth of investigation of a profile is defined as the depth up to which the inverted model obtained does not depend on how the inversion is implemented (Oldenburg and Yaoguo, 1999). We derived this depth for each profile to determine the depth to which the models obtained were reliable.

A point to be taken into account is the trend of the gas pipeline. It corresponds to a middle-pressure system and the diameter of the pipe is 20 cm. The pipeline runs embedded at a depth of 0.5 m in a direction perpendicular to the ravine, at approximately 3 m from the chamber (see Fig. 3). In a previous paper

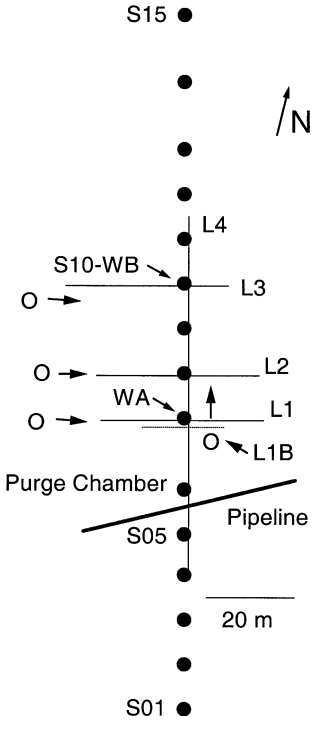

Fig. 3. Location of the soundings. L1, L2, ... indicate the dipole–dipole locations. S01, S05, ... the Wenner centers. WA and WB indicate the location of the two control wells. The O → indicates the origin of the profiles and direction of increasing station values.

(Osella et al., 2000), the effect of an embedded pipeline on geoelectrical soundings was estimated. For this kind of pipe, the effect becomes negligible at approximately 2 m apart from it, then the profiles were located at distances large enough to avoid its influence.

4. Profiles perpendicular to the ravine axis

Four dipole–dipole profiles were performed perpendicular to the ravine axis as shown in Fig. 3. The first three (L1, L2, and L3) had a length of 40 m with a 1 m separation spacing between electrodes and a maximum separation for $n = 9$ (see Fig. 2a). L1 and L3 intersected the well locations, WA and WB, respectively, while L2 was in between them, 10 m apart from L1. The wash slope of the ravine goes downward in the direction from L1 towards L3. The first and last 6 m, approximately, of these profiles sloped upwards due to the sides of the ravine. The data collected from the three lines are shown in Fig. 4; in this figure, the topographic corrections for each line are also shown. The resistivity sections obtained inverting the data are shown in Fig. 5a, b and c for L1, L2 and L3, respectively. The misfit for each sounding is shown in Fig. 6. A good fitting implies not only low values but also a random distribution of

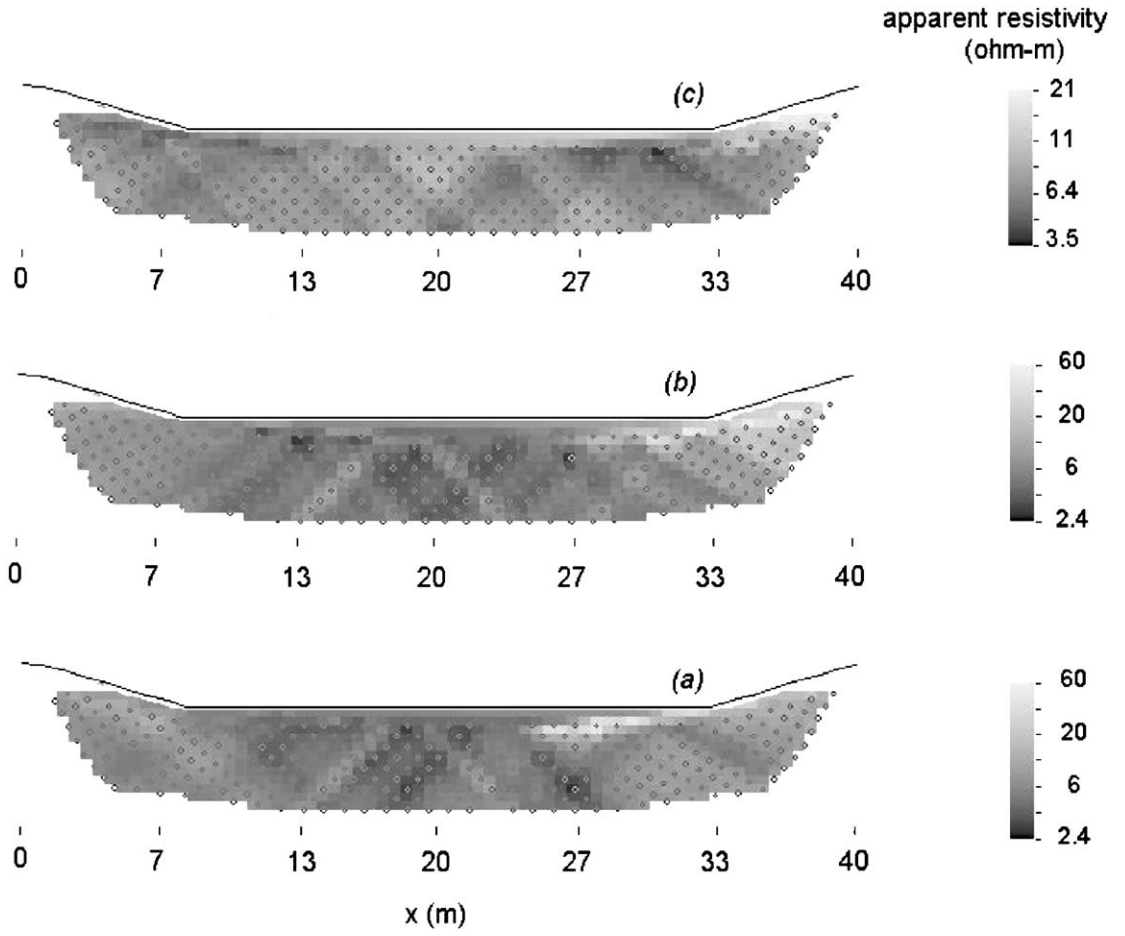

Fig. 4. Apparent resistivity data with topographic corrections for the dipole–dipole profiles perpendicular to the ravine axis. (a) L1 profile, (b) L2 profile, and (c) L3 profile.

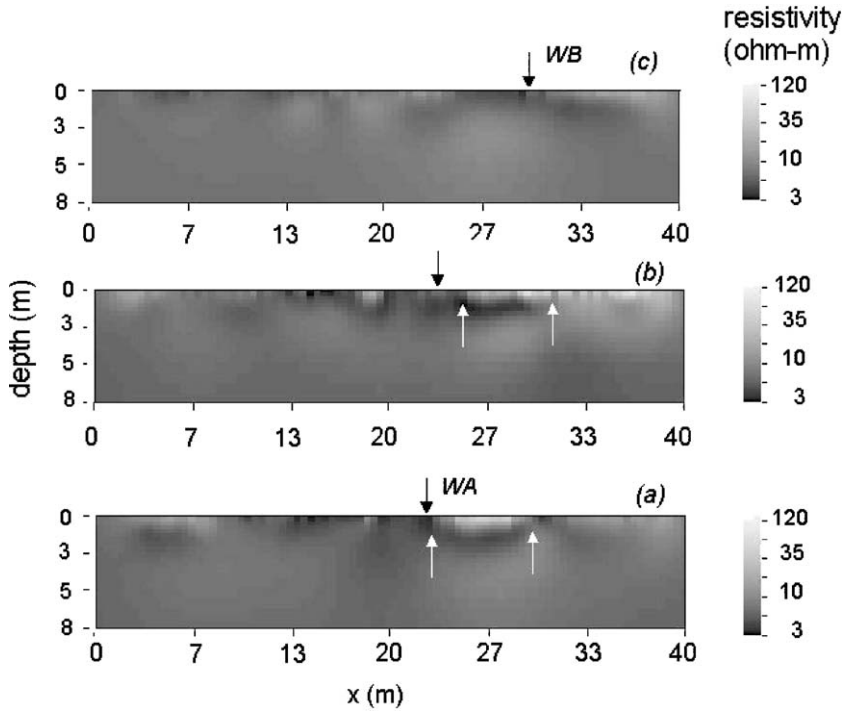

Fig. 5. Electrical imaging obtained from the 2D inversion of (a) L1 data, (b) L2 data, and (c) L3 data. The black arrow in (b) indicates the location where the line connecting WA and WB cuts L2, the white arrows delimit the anomalous zone.

the errors. The misfits shown in Fig. 6 for the three lines satisfy these conditions, supporting the confidence of the results.

From Fig. 5a, we see that the inversion model at L1 presents important lateral variations. Both ends of the profile, the first and last 6 m, approximately, have a more resistive superficial layer (about 20 Ω m) due probably to cover material (sediments) as these zones correspond to the ravine side slopes. As we move towards the center of the profile, the soil is more conductive: about 5 Ω m. The behavior of the soil between 20 and 30 m from the origin (white arrows in Fig. 5a) is quite different (see also Fig. 4a). There is a shallow zone of resistivity higher than the medium, between 60 and 120 Ω m, surrounded by a very conducting layer of less than 3 Ω m. That higher resistive layer extends to a maximum depth of 2 m and decreases to less than 1 m where the sounding well WA is located. Below these layers, at approximately 3 m, the resistivity increases slightly up to 10 Ω m, and decreases towards both sides of the profile.

L2 shows a similar behavior, but the shallow resistive layer is more conductive, as seen in Fig. 5b. The black arrow indicates the point where the line connecting the two sounding wells cuts this profile. Right to this point, as on L1, there is a more resistive superficial zone (of approximately 100 Ω m) contained by a more conductive layer. The resistive zone is narrower than on L1 and shifted about 2 m with respect to the line connecting both wells (black arrow in Fig. 5b). There is another resistive zone to the left of the black arrow, but it is at most of 20 Ω m. The first 6 or 7 m of the line show a more resistive cover, coinciding with the higher topographic level.

L3, on the other hand, shows a very different behavior (Fig. 5c). In this case, the center of the profile was displaced with respect to the ravine axis (see Fig. 3). The central point was located at the lowest topographic point. The soil on this line is in general more uniform and conductive than on L1 and L2, in agreement with the borehole data (the location of WB is shown in this figure).

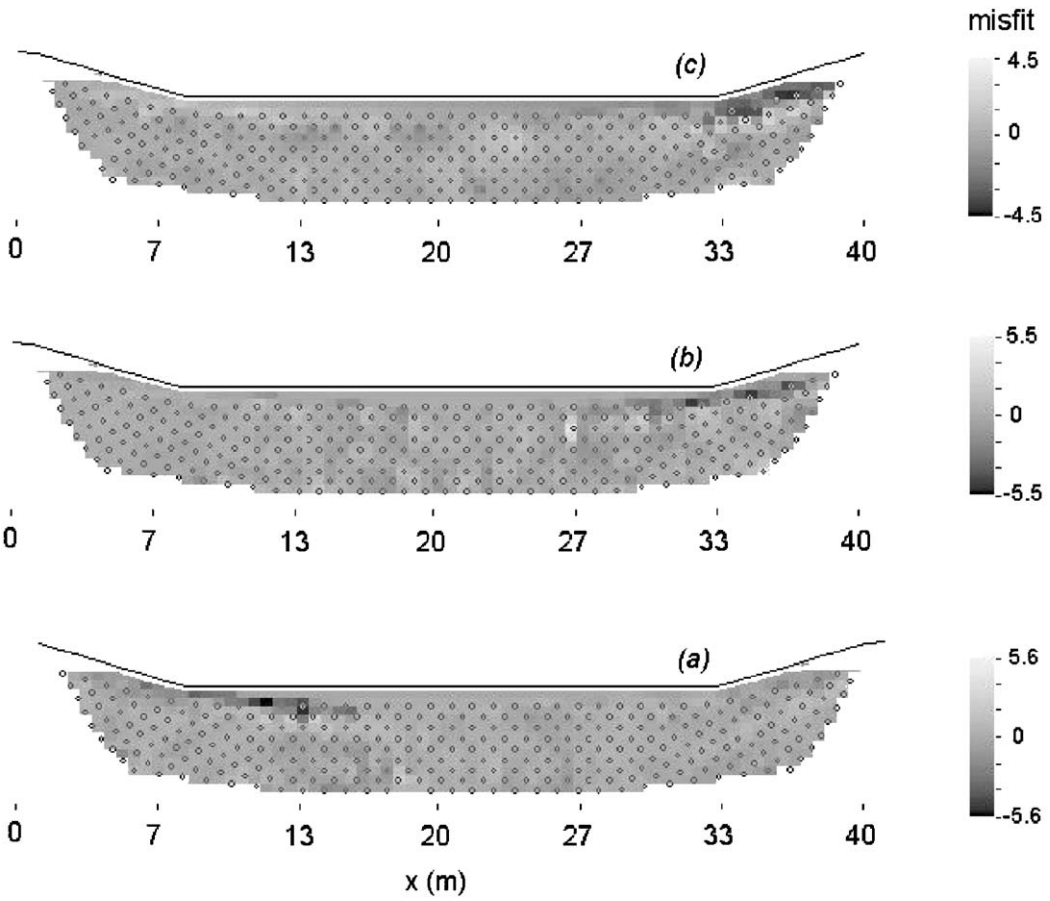

Fig. 6. Misfit (difference between the observed and predicted data, normalized to the standard deviation) corresponding to the inversion of: (a) L1, (b) L2, and (c) L3.

From the results on L1, L2, and L3, we see that the shallow resistive zone has a lateral extent of 7 m on L1, is reduced to 2 m at L2 and is absent at L3. Comparing the resistivity model obtained from L1 with the control well (WA) data, we conclude that the shallow zone in L1 and L2 can be correlated with the contaminated lens.

To better determine the anomalous zone detected on L1, a fourth dipole–dipole profile was performed at the same site as L1 (L1B, see Fig. 3), with better resolution, but less extent. L1B is centered on the same site as L1. It has an extent of 20 m with a 0.5 m spacing between electrodes and a maximum n of 11. This shorter section was flat, so no topographic correction was needed. In Fig. 7a, the resistivity model obtained from the inversion of the data is shown; also the resistivity model for the same zone obtained from L1 is added for comparison (Fig. 7b).

From the inversion of L1B data (Fig. 7a), we can infer that the *lateral* resistive superficial zone has a transverse extent between 6 to 7 m. Underlying this resistive zone we see a more conductive zone and below it the presence of a layer that is a little more resistive (from 2–3 to 9–12 Ω m). This is in *agreement* with the model results obtained from L1 (see Fig. 7b). Although there is the possibility of a leak to explain the deeper resistive layer, from Fig. 7 we see that the conductive zone confines the more resistive superficial zone making this possibility unlikely.

Also there is a narrow superficial conductive layer in Fig. 7a of thickness no more than 0.5 m. The origin

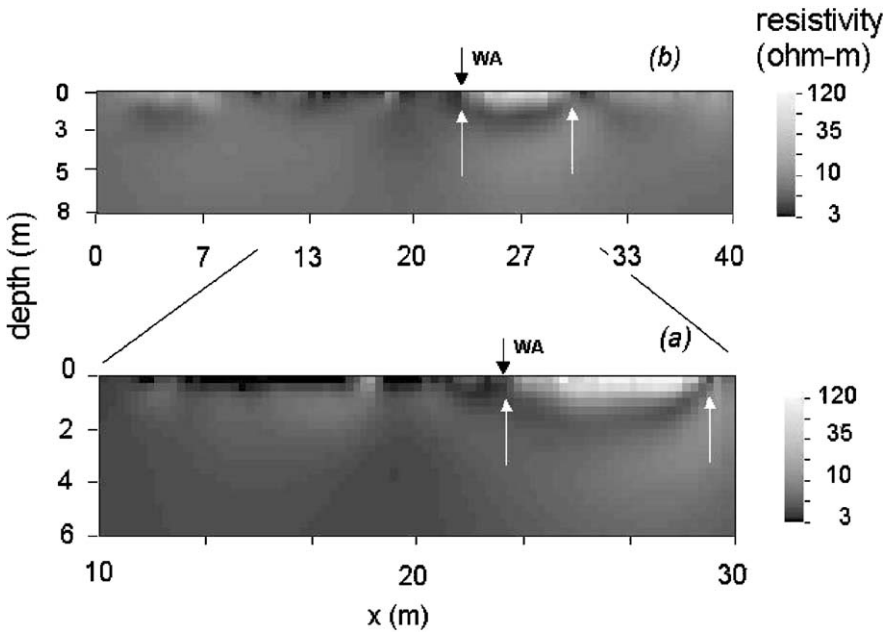

Fig. 7. Electrical imaging obtained from the 2D inversion of L1B data (a), and the electrical imaging obtained from L1 data at the same sector (b). The white arrows delimit the anomalous zone.

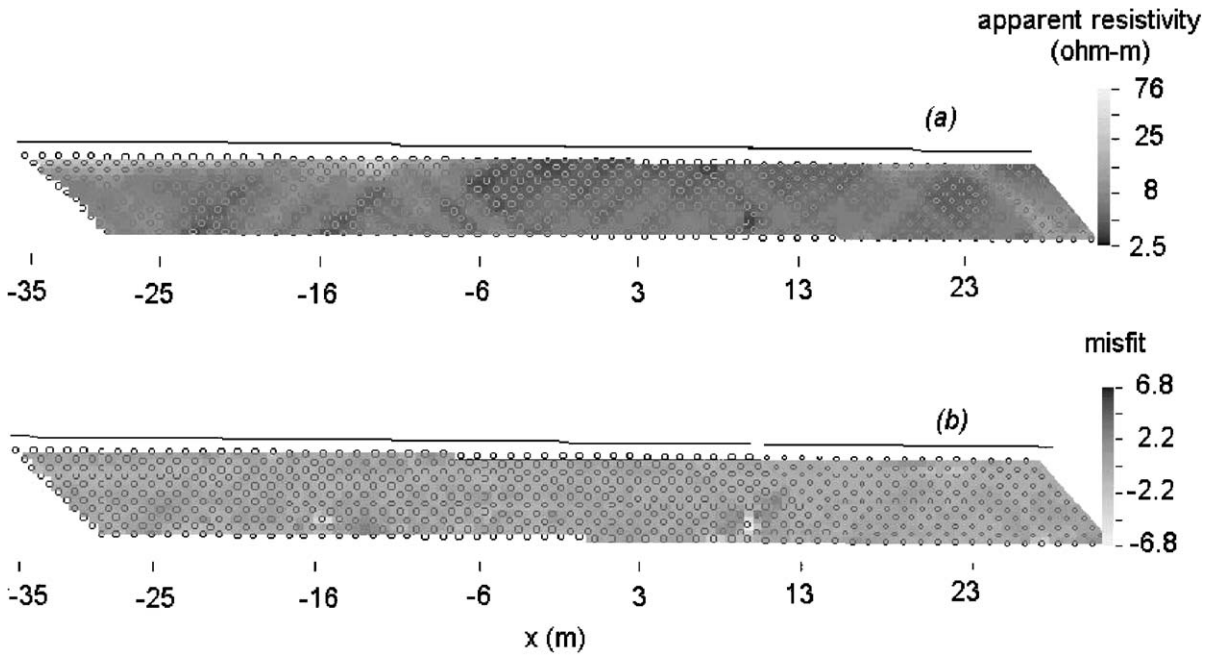

Fig. 8. Dipole–Dipole line L4. (a) Apparent resistivity data including topographic corrections. (b) Misfit (see caption Fig. 6) corresponding to the inversion of this data.

of this layer is probably due to clay material related to the dry riverbed.

5. Soundings parallel to the ravine axis

To define the longitudinal extent of the contaminated zone, an 80 m long dipole–dipole sounding along the ravine axis (L4) was performed. Along this line, 15 *Wenner vertical soundings* were also performed to study the soil structure in depth (Figs. 1 and 3).

The dipole–dipole line was surveyed with a 1 m separation between electrodes and a maximum n of 11. It crossed the purge chamber and the two control wells. The apparent resistivity pseudosection data obtained on this line is shown in Fig. 8a; due to the large amount of data involved we show only selected sections of data and the corresponding misfit (Fig. 8b). The resistivity model obtained inverting the data is shown in Fig. 9. Topography was taken into account as there is a smooth slope along this direction. In Fig. 9a the whole resistivity section is shown, while in Fig. 9b we show an amplification of the first 36 m of the line.

In Fig. 9a, we see that the resistivity model obtained from L4 reproduces the soil pattern model obtained near WA by means of the transverse L1 and L1B lines. Between the purge chamber and the control well WA there is the same layer distribution. The extent in this direction of the superficial resistive layer is of 10 m. From the purge chamber up-slope towards the beginning of the profile ($x = -40$ m), there is another superficial resistive cover of the same resistive order as the one detected between the purge chamber and WA. To evaluate the possibility of a contaminant flow in this direction, which in fact would run along an ascending topographic slope, we showed a zoom view of the first 36 m of the electrical model obtained from L4 (Fig. 9b). In this figure, we see with better resolution, that the resistive layer between the purge chamber and WA *is not connected to the second zone*, between the purge chamber and the beginning

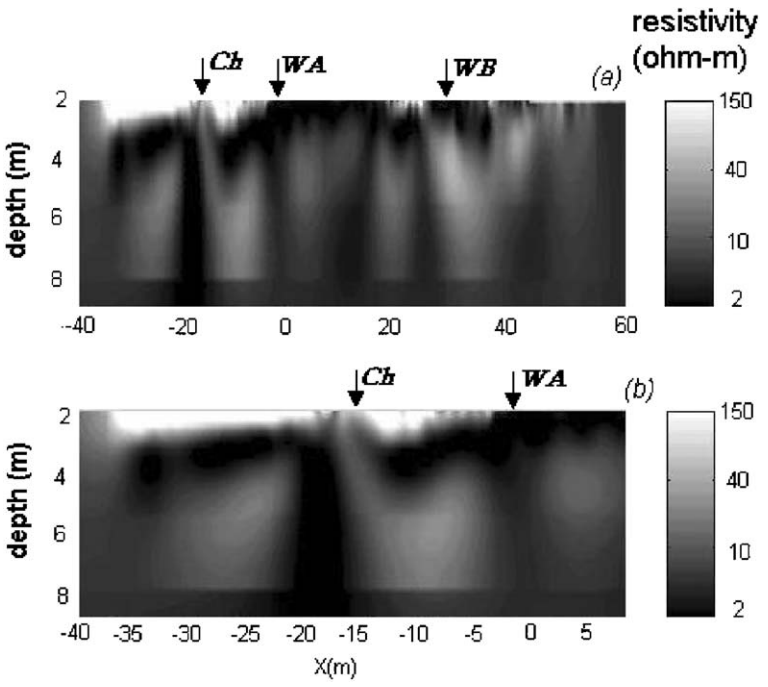

Fig. 9. Electrical imaging obtained from the 2D inversion of L4 data (a), and the same data amplified between −40 and 5 m from the origin (b). The location of the chamber (Ch), and wells WA and WB are also shown.

of the profile. As the topographic slope is descendent along the line, we conclude that this resistive *layer is disconnected from the contaminated zone* seen at the well.

Along the same direction of L4, 15 Wenner in-line soundings (S01 to S15, Fig. 3) were performed. For each profile, 24 different spacings were used, varying between 0.25 and 60 m. The data obtained are presented in the form of a pseudosection which shows the apparent resistivity in depth along this direction (Fig. 10a). In Fig. 10b, we show the resistivity soil model obtained from the 2D inversion of these data.

This model has less lateral resolution than the model obtained from the dipole–dipole configuration, particularly in the first few layers, as the profiles were performed at about 4 m apart from each other, but it resolves the deeper layers, up to 30 m. The first 10 m give average results similar to the ones obtained from L4. Except for the first meters from the beginning, the resistive values are low, between 2 and 14 Ω m. The higher resistive values, although they do not exceed 14 Ω m, are found towards the end of the sounding in the lower region.

6. Joint inversion of Wenner and dipole–dipole data

The model results obtained from the inversion of the dipole–dipole and Wenner data presented different features; due to the length of the spread used in the deployments, the dipole–dipole gave good lateral resolution but low penetration, in spite of the larger value of n (see Fig. 2a), while the Wenner array, carried out by performing vertical soundings, defined the soil in depth but with low lateral resolution of the shallow layers. To improve the final electrical model, we tested the joint inversion of both sets of data. In Fig. 11, we show the resistivity model obtained. The model results indicate that the details in the shallow layers remain while there is more definition in the deeper layers.

When we analyzed the depth of penetration for each set separately, we found that using the Wenner configuration the depth of investigation was 20 m (see Fig. 10b) while for dipole–dipole was 8 m (Fig. 9). Although the dipole–dipole configuration gives very good shallow lateral resolution it does not have high depth penetration, at least with the spacing required to

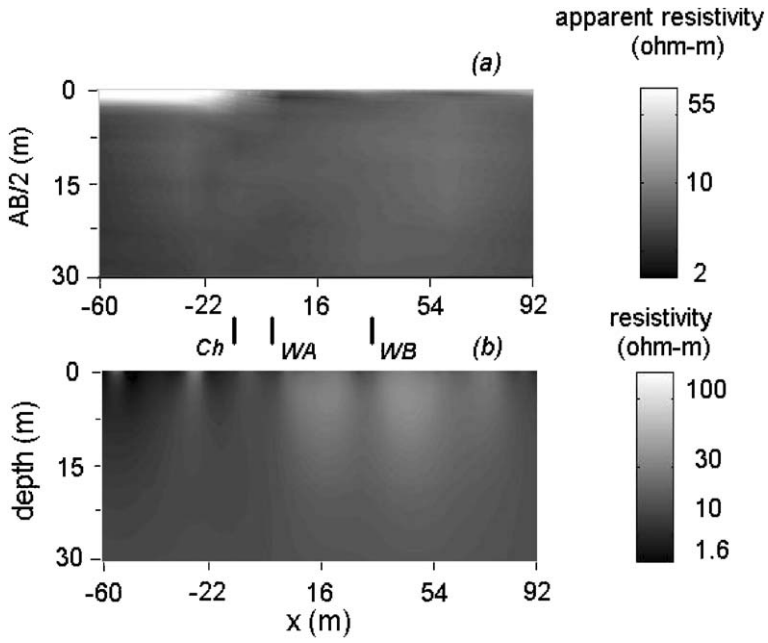

Fig. 10. Wenner soundings. (a) Apparent resistivity pseudosection data. (b) Electrical imaging obtained from the 2D inversion of the Wenner data. The location of the chamber (Ch), and wells WA and WB are also shown.

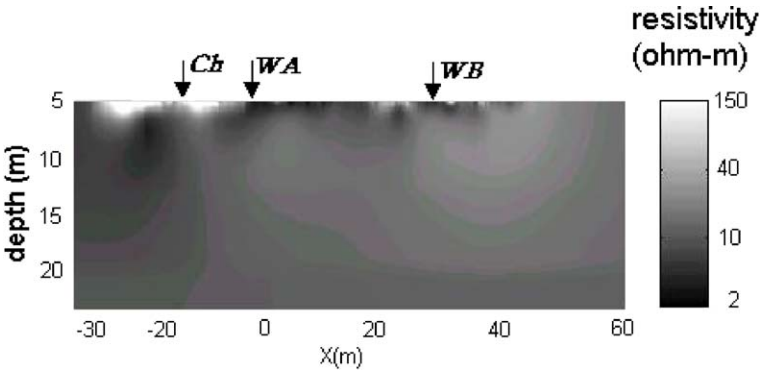

Fig. 11. Electrical imaging obtained from the 2D combined inversion of the L4 data and Wenner data.

resolve and characterize the shallow structure. For the joint Wenner and dipole–dipole inversion model a depth of 25 m was found. This indicates that the joint inversion reaches a greater depth of investigation.

Summing up, we can conclude that the joint inversion of Wenner and dipole–dipole data gives a model with deeper penetration than both dipole–dipole and Wenner alone, and also gives better shallow lateral resolution than Wenner alone, i.e., it gives a model with good lateral resolution and also with a greater depth of investigation.

7. Discussion and conclusions

From the inversion of the different profiles, we have delineated a contaminated zone of approximately 6 m of transverse extent and 16 m in the longitudinal direction (the direction of the natural slope) between the purge chamber and the sounding well WA. The identification of this zone with a zone with contaminants is based on the well data and the resistivity contrasts found. It was found also that this contamination plume is surrounded by a clay soil, which prevents a major *migration*.

Regarding the description of the soil, from L4 we determined that there is a resistive shallow layer along the first 10 m of this profile. The models obtained from the dipole–dipole data (Fig. 9) and the Wenner data (Fig. 10b) allow us to confirm that this is a covering layer, and that this zone is not connected to the plume due to the presence of an intermediate impermeable clay zone. Although the possibility of diffusion by a fissure cannot be completely ruled out, it seems to be highly improbable if we also take into account the direction of the topographic slope.

We observe that where lines L1 and L4 cross, below the plume in the direction of both L1 and L4 there is a more resistive layer between 4 and 9 m. Although there is not too much contrast, it may be due to a contaminant filtration. Below the well WB there is also an anomalous zone, but from L4 we see that it is isolated from the purge chamber. This assumption seems to be confirmed by the facts that it required several days for the water to ascend and that no contaminants were found, neither flowing nor dissolved in water.

One of the interesting results that we obtained from the electrical tomographies, constrained by the control well data, is the resistive characteristic of the contaminant plume. This result is in fact in agreement with previous studies performed at different purge chambers located on the same pipeline trend (Osella et al., 2002; Alvin, 2002). As we pointed out at the beginning of this work, the electrical signature of a contaminant plume depends on the biodegradation process occurring in the contaminated lens. One of the causes to explain the resistive nature of this plume could be that it is a rather young spill, in which the biodegradation process is at its beginning. But local information indicated that the first hints of contamination of the groundwater were reported at least 4 years before the present study; then it should not be a young spill, at least according to some authors (e.g., Shevnin et al., in press). On the other hand, the chemical analysis showed that waters were rich in bicarbonates and

presented low salinity (Grizinik, 2000). The low salinity may stand for a low concentration of dissolved solids in this aquifer, which is a possible indicator that enhanced mineral dissolution is not taking place. This should imply that degradation, if occurring, is taking place at a very low rate. In this manner, the environment could be the possible cause of the absence of biodegradation and the consequent resistive characteristic of the plume. Some authors (e.g., Aal et al., in press) have said that it is not clear yet how the presence of clays may influence the biogeochemical reactions. In the region where we have performed the studies, the water table is contained in porous lens embedded in a clay environment; then it may be that clays act in some way delaying chemical reactions. Up to now there is not an answer to explain this behavior and it remains open for further investigation.

The methodology applied to solve the problem proved to be successful to map the contaminated zone. In a previous work (Osella et al., 2002), a 1.5-m-thick contaminant layer located at approximately 8 m depth was mapped. In that study, we applied Wenner arrays to delineate the extent and location of the contaminant lens, and afterwards we carried out selected dipole–dipole profiles to derive the characteristics of the shallow layers, as required for the future remediation. In the present case, we had to deal with a thinner lens, about 0.50 m of gasoline, and rather shallower, at 1 or 2 m depth. Also, a well-defined topographic slope required a mapping of the deeper layer to be able to estimate the development of the contamination and predict the possible flow through the descending slope. The first transversal four dipole–dipole lines allow us to find the lateral extent as well as the depth of the contaminated zone. The thickness of this resistive layer associated with the contaminants, about 1 to 2 m, is larger than the expected value, according to the well data, but in this case this can be explained if it is taking into account that, if there is a gasoline layer floating on the water table, this water must contain also dissolved gasoline, which produce, in this case, an increase in the resistivity of the whole zone involved.

The longitudinal dipole–dipole profile allowed us to localize the plume, which appeared to be confined by a conducting medium associated with clay materials. This result was confirmed by the Wenner array results. To improve the reliability of the resulting models, we performed joint inversion of Wenner and dipole–dipole data. Analysis of the depth of penetration showed that it is larger when all the data are considered together. Finally, we can conclude that this procedure gave us a final model with high lateral resolution to characterize the extent of the anomalous zone and also better definition in depth, enabling us to conclude that this anomalous zone associated with the gasoline was confined by impermeable clay environment, which prevents its flow to other regions.

Acknowledgements

This work was supported by the University of Buenos Aires and Agencia Nacional de Promoción Científica y Tecnológica (ANPCyT). We thank Dr. Atekwana for her useful comments.

References

Aal, G.Z.A., Werkema, D., Sauck, W., Atekwana, E., 2002. Geophysical investigation of vadose zone conductivity anomalies at a former refinery site, Kalamozoo. 14 Annual Meeting EEGS, Denver, Colorado, 2001. Published on CD.

Alvin, A., 2002. Geophysical studies along Los Perales pipeline trend, (personal communication).

Atekwana, E.A., Sauck, W.A., Werkema, D.D., 2000. Investigations of geoelectrical signatures at a hydrocarbon contaminated site. J. Appl. Geophys. 44, 167–180.

Benson, A.K., Payne, K.L., Stubben, M.A., 1997. Mapping groundwater contamination using dc resistivity and VLF geophysical methods. Geophysics 62, 80–86.

Buselli, G., Lu, K., 2001. Groundwater contamination monitoring with multichannel electrical and electromagnetic methods. J. Appl. Geophys. 48, 11–23.

Endres, A.L., Greenhouse, J.P., 1996. Detection and monitoring of chlorinated solvents by thermal neutron logging. Ground Water 34, 283–292.

Fetter, C., 1993. Contaminant Hydrogeology. Prentice Hall, New Jersey.

Grizinik, M., 2000. Geohidrología del área noroeste de Santa Cruz, Argentina, Universidad San Juan Bosco Ed. (internal report).

Oldenburg, D.W., Li, Y., 1994. Inversion of induced polarization data. Geophysics 59, 1327–1341.

Oldenburg, D.W., Yaoguo, L., 1999. Estimating depth of investigation in dc resistivity and IP surveys. Geophysics 64 (2), 403–416.

Oldenburg, D.W., McGillivary, P.R., Ellis, R.G., 1993. Generalized subspace method for large scale inverse problems. Geophys. J. Int. 114, 12–20.

Osella, A., Chao, G., Sánchez, F., 2000. How to detect buried

structures through electrical measurements. Am. J. Phys. 69 (2), 1–7.

Osella, A., de la Vega, M., Lascano, E., 2002. Characterization of a contaminant plume due to a hydrocarbon spill using geoelectrical methods. J. Env. Eng. Geophys. 7 (2), 78–87.

Reynolds, J., 1998. An Introduction to Applied and Environmental Geophysics. Wiley, New York.

Sauck, W., 1998. A conceptual model for the geoelectrical response of LNAPL plumes in granular sediments. Proc. of the Symposium on the Application of Geophysics to Engineering and Environmental Problems (EEGS), pp. 805–817.

Sauck, W.A., 2000. A conceptual model for the geoelectrical response of LNAPL plumes in granular sediments. J. Appl. Geophys. 44, 151–165.

Sauck, W., Atekwana, E.A., Bermejo, J.L., 1998. Characterization of a Newly Discovered LNAPL Plume at Wurtsmith AFB, Oscoda. 11 Annual Meeting EEGS, Chicago, Illinois, pp. 399–408.

Shevnin, V., Ryjov, A., Nakamura, E., Sanchez, A., Korolev, V., Mousatov, A., 2002. Study of oil pollution in Mexico with resistivity sounding. 15 Annual Meeting EEGS, Las Vegas, Nevada, 2002. Published on CD.